Fracture via a sequence of events: a saw-tooth softening model

J.G. Rots
Delft University of Technology, Delft, The Netherlands

S. Invernizzi
Politecnico di Torino, Torino, Italy. Also research fellow at TUDelft.

B. Belletti
University of Parma, Parma, Italy. Also research fellow at TUDelft.

ABSTRACT: The sequentially linear analysis is a robust alternative to non-linear finite element analysis of structures when bifurcation, snap-back or divergence problems arise. The load-displacement response is captured by a series of linear analyses as a sequence of 'events'. Every 'event' is a scaled critical states corresponding to the reaching of some peak of some saw-tooth for some softening element. In the present paper, the approach is extended with a rippled saw-tooth curve which applies to any stress-strain diagram, included compression nonlinearity and yielding of reinforcement. Several RC structural examples demonstrate that both sharp snap-backs as well as ductile failures can be handled correctly.

1 INTRODUCTION

Non-linear finite element analysis is becoming a common tool for studying the behavior of reinforced concrete structures. Over the past years, techniques for non-linear analysis have been enhanced significantly via improved solution procedures, extended finite element techniques and increased robustness of constitutive models. Nevertheless, problems remain, especially when cracking and crushing in real-world structures is analyzed. The load-displacement response of RC beams, plates, shells and spatial structures often shows a number of local peaks and snap-backs or valleys associated with brittle cracking [1] and subsequent stress redistribution. In simulating this behavior, one has to use softening models. Unfortunately, this involves negative tangent stiffness which may lead to numerical instability and divergence of the incremental-iterative procedure. To try and solve such problems, users have to resort to arc-length or indirect control schemes [2]. For practicing engineers this is cumbersome and often inadequate when the bifurcations are multiple, the peaks irregular or the snap-backs sharp [3]. These problems are independent of the type of smeared crack formulation adopted, either decomposed-strain, total-strain, damage or plasticity based crack models. In this contribution, an alternative method is adopted [4]. The softening diagram of negative slope is replaced by a saw-tooth diagram of positive slopes. The incremental-iterative Newton method is replaced by a series of linear analyses using a special scaling technique with subsequent stiffness/strength reduction per critical element. It will be shown that

this 'event-by-event' strategy is robust and reliable. The advantage is that there is no such thing as 'negative incremental stiffness', as the secant linear (saw-tooth) stiffness is always positive. The analysis always 'converges'. Mesh-size objectivity is achieved by keeping the fracture energy invariant.

In the paper, details are provided concerning the saw-tooth implementation of the basic materials in RC structures, namely concrete and steel both in tension and compression. Subsequently, various reinforced structures are considered: the reinforced tension-pull specimen, two simply supported deep beams, and one deep beam on three supports. In all cases, the response shows local peaks and snap-backs associated with the subsequent development of primary cracks starting from the rebar. Comparisons between incremental-iterative solutions and sequentially linear solutions are given and the behaviour is interpreted in terms of crack spacing and crack width. The model is demonstrated to be stable and robust and therefore appealing to practising RC engineers.

2 OVERALL EVENT-BY-EVENT PROCEDURE

The locally brittle snap-type response of many RC structures inspired the idea to capture these brittle events directly rather than trying to iterate around them in a Newton-Raphson scheme. A critical event is traced and subsequently a secant restart is made from the origin for tracing the next critical event. Hence, the procedure is sequential rather than in-

cremental. The sequence of critical 'events' governs the load-displacement response. To this aim, the softening diagram is replaced by a saw-tooth curve and linear analyses are carried out sequentially [4]. The global procedure is as follows. The structure is discretized using standard elastic continuum elements. Young's modulus, Poisson's ratio and initial strength are assigned to the elements. Subsequently, the following steps are sequentially carried out:

- Add the external load as a unit load.
- Perform a linear elastic analysis.
- Extract the 'critical element' from the results. The 'critical element' is the element for which the stress level divided by its current strength is the highest in the whole structure.
- Calculate the ratio between the strength and the stress level in the critical element: this ratio provides the 'global load factor'. The present solution step is obtained rescaling the 'unit load elastic solution' times the 'global load factor'.
- Increase the damage in the critical element by reducing its stiffness and strength, i.e. Young's modulus E and tensile strength f_t, according to a saw-tooth constitutive law as described in the next section.
- Repeat the previous steps for the new configuration, i.e. re-run a linear analysis for the structure in which E and f_t of the previous critical element have been reduced. Trace the next critical sawtooth in some element, repeat this process till the damage has spread into the structure to the desired level.

The way in which the stiffness and strength of the critical elements are progressively reduced constitutes the essence of the model. In other words, it is necessary to provide a saw-tooth approximation of the constitutive stress-strain relation [4-6]. In the present paper a new generalized tooth size approach is presented, which allows for a straightforward unification of saw tooth constitutive laws for concrete in tension, concrete in compression and steel in tension and compression.
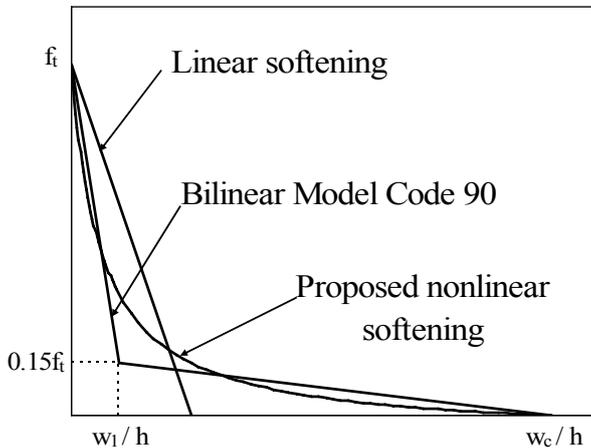
Figure 1. MC90 cohesive law (bilinear); linear softening and nonlinear softening with equal strength and fracture energy.

3 SAW-TOOTH CONSTITUTIVE LAWS FOR RC

3.1 *Saw-Tooth Laws for Concrete in Tension*

The behavior of concrete in tension is correctly described by the Model Code 90 (MC90) bilinear relation [6]. A linear relation can be also adopted (Fig. 1), which preserves the tensile strength and the fracture energy, though this choice turns out to overestimate the immediate post peak behavior, and to underestimate the ultimate strain.

3.2 *Saw-Tooth Nonlinear Tension Softening*

The cohesive relation of the MC90 provides the tensile stress σ transmitted by the crack as a function of the crack opening w in the following way:

$$
\begin{cases}
\sigma = f_t \left(1 - 0.85 \dfrac{w}{w_1} \right) \Rightarrow 0.15 \cdot f_t \le \sigma \le f_t \\
\sigma = \dfrac{0.15 \cdot f_t}{w_c - w_1} (w_c - w) \Rightarrow 0 \le \sigma < 0.15 \cdot f_t
\end{cases}
\tag{1}
$$

The crack opening w_1 and the ultimate crack opening w_c depend of the tensile strength and fracture energy:

$$
\begin{cases}
w_c = \alpha_F \dfrac{G_F}{f_t} \\
w_1 = 2 \dfrac{G_F}{f_t} - 0.15 \cdot w_c
\end{cases}
\tag{2}
$$

In absence of experimental data, the concrete fracture energy can be estimated as a function of the characteristic compressive strength f_{ck}:

$$
G_F = G_{F0} \left(\frac{f_{cm}}{10} \right)^{0.7}
\tag{3}
$$

Both α_F and the basic fracture energy of concrete G_{F0} are functions of the maximum aggregate size.

The MC90 bilinear expression has been recently modified by Belletti, Cerioni and Iori [7] in order to have a continuous function, which is better for our purpose. This expression reads as follows:

$$
\sigma = f_t \left(1 - \frac{w}{\left(1 - \dfrac{w_1}{\delta \cdot w_c} \right) \cdot w + \dfrac{w_1}{\delta}} \right)
\tag{4}
$$

where $\delta = 1.75$ is a parameter which guarantees that the area underneath the curve (i.e. the fracture energy) remains unchanged.

The following step is to implement the above cohesive curve into a smeared-crack total strain formulation. Therefore, it is necessary to smear the crack

opening w over the crack band width or element size h, and to express the crack strain as the difference between the total strain and the elastic part as follows:

$$\begin{cases} w = \varepsilon_{cr} \cdot h \\ \varepsilon_{cr} = \varepsilon - \dfrac{\sigma}{E} \end{cases} \tag{5}$$

Eq. (5) can be substituted in eq. (4), providing the following quadratic expression:

$$\sigma = f_t \left(1 - \dfrac{\varepsilon - \dfrac{\sigma}{E}}{\left(1 - \dfrac{w_1}{\delta \cdot w_c}\right) \cdot \left(\varepsilon - \dfrac{\sigma}{E}\right) + \dfrac{w_1}{\delta \cdot h}} \right). \tag{6}$$

After some algebraic manipulation, and since only the lower root of the above equation is physically meaningful, the stress strain relation in terms of total strain is the following:

$$\begin{cases} \sigma = E \cdot \varepsilon & 0 \le \varepsilon \le f_t/E \\ \sigma = \dfrac{B - \sqrt{B^2 - 4 \cdot A \cdot C}}{2 \cdot A} & f_t/E < \varepsilon \le w_c/h \end{cases} \tag{7}$$

with:

$$\begin{cases} A = (\delta \cdot w_c \cdot h - w_1 \cdot h) \\ B = [E(\delta \cdot w_c \cdot h - w_1 \cdot h)\cdot \varepsilon + E \cdot w_1 \cdot w_c - f_t \cdot w_1 \cdot h] \\ C = E \cdot f_t (w_1 \cdot w_c - w_1 \cdot h \cdot \varepsilon) \end{cases} \tag{8}$$

Eq. (7) can now be adopted as a 'mother curve' for the construction of the saw tooth approximation.

Since the softening tail is nonlinear, implementation of previous saw-tooth approaches [5-6] is not straightforward. Therefore, a more general approach is proposed. The main idea is to define a narrow band across the 'mother curve', obtained by uplifting and lowering the softening curve with some quantity proportional to the tensile strength (Fig. 2). The uplifted softening function will be the following:

$$\sigma^+ = \dfrac{B - \sqrt{B^2 - 4 \cdot A \cdot C}}{2 \cdot A} + p \cdot f_t \tag{9}$$

where p is a percentage of the strength. The intersection between the generic i secant elastic branch and the softening tail, i.e. the arbitrary tooth peak, is provided by the following equation:

$$E\varepsilon^+ = \dfrac{B - \sqrt{B^2 - 4 \cdot A \cdot C}}{2 \cdot A} + p \cdot f_t \tag{10}$$

After some algebraic manipulation, Eq. (10) can be solved with respect to the strain, giving again a quadratic expression, which provides only one physically meaningful solution:

$$\varepsilon_i^+ = \dfrac{-b + \sqrt{b^2 + 4 \cdot a \cdot c}}{2 \cdot a} \tag{11}$$

The corresponding strength can be obtained easily by:

$$f_{ti}^+ = E_i \cdot \varepsilon_i^+ \tag{12}$$

Every time that the element is critical, according to the overall 'event-by-event' procedure, the stiffness and the strength of the element must be reduced. The rule to apply is:

$$E_{i+1} = \dfrac{f_{ti}^+ + 2pf_t}{\varepsilon_i^+} = \dfrac{f_{ti}^-}{\varepsilon_i^+}; \quad 0 \le i \le N \tag{13}$$

where f_{ti}^- is the interception of the secant stiffness with the lowered softening curve. This rule can be applied sequentially, replacing the initial softening mother curve by the saw-tooth approximation (Fig. 2).
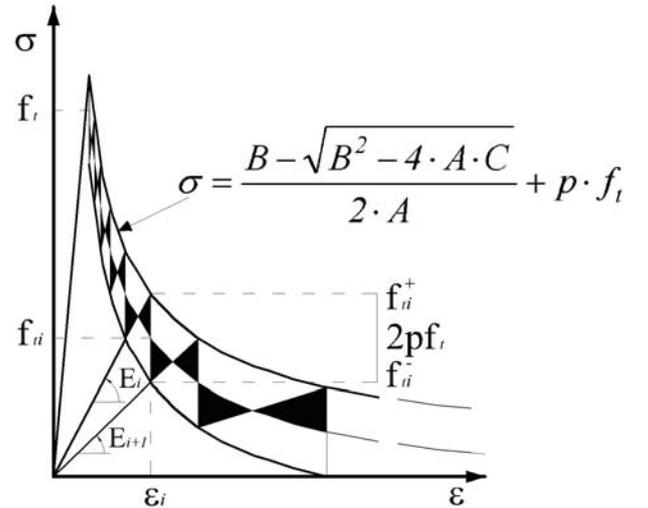
Figure 2. Generic intersection with the uplifted softening curve and saw-tooth constitutive law.

Contrarily to previous procedures [5-6], the height of each ripple is constant here and equal to twice the uplift amount. The number of teeth of the saw-tooth approximation is equal to the number of repetitions which can be performed until f_{ti}^- becomes negative, i.e.:

$$N = 1 + max\left(i : f_{ti}^- > 0\right) \tag{14}$$

Note that $i=N$ corresponds to complete damage. Thanks to the fact that every ripple has the same height, the black triangles in Fig. 2 are two-by-two equal to each other. Therefore, the area under the

saw-tooth curve is always equal to the fracture energy divided by the crack band width, regardless the element size and/or the number of teeth in the discretization. This provides the saw-tooth approximation to be mesh-size objective. The above procedure is general and applies to any arbitrary total strain formulation.

3.3 Saw-Tooth Laws for Concrete in Compression

The compressive behavior of concrete can be modeled by the simplified EC2 bi-linear stress-strain relation [9], where $\varepsilon_{c3} = -1.75^0/_{00}$ and $\varepsilon_{cu3} = -3.5^0/_{00}$ respectively, for characteristic cylindrical compressive strengths up to 50 MPa.
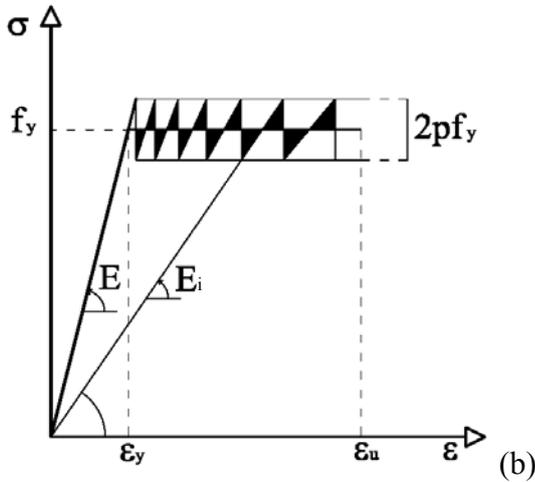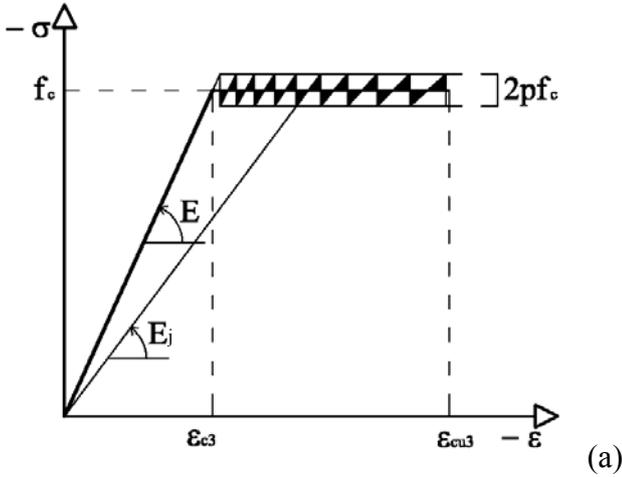
Figure 3. Mother curve and saw-tooth approximations: concrete in compression (a); steel in compression and tension (b).

This case exhibits a plastic behavior of constant stress level instead of a softening degradation (Fig.3a). Moreover, the EC2 relation is already expressed in terms of total strain. The uplifted post peak curve is obtained as follows:

$$\sigma^+ = (1 + p)f_c \tag{15}$$

Where, f_c is the compressive strength and p the percentage of strength uplifting. The intersection between the generic j secant elastic branch and the plastic plateau, provides the following equation:

$$E_j \varepsilon_j^+ = (1 + p)f_c \tag{16}$$

Therefore, analogously to Eq. (11), the strain becomes:

$$\varepsilon_j^+ = \frac{(1 + p)f_c}{E_j} \tag{17}$$

Note that we use j to quantify the level of damage in compression, since i was used for damage in tension. The updated (i.e. degradated) Young's modulus becomes:

$$E_{j+1} = \frac{(1 + p)f_c - 2pf_c}{\varepsilon_j^+} = \frac{f_{ci}^-}{\varepsilon_j^+} = E_j \frac{1 - p}{1 + p}; \tag{18}$$

$$0 \le j \le N$$

A slightly different criterion is adopted to determine the number of teeth; in fact it turns out to be necessary to limit the ultimate strain of the saw-tooth diagram according to the mother curve:

$$|\varepsilon_N| \le |\varepsilon_{cu3}| \Rightarrow \left| \frac{\frac{f_c(1 + p)}{E}}{\left(\frac{1 - p}{1 + p}\right)^N} \right|. \tag{19}$$

Finally, the number of teeth becomes:

$$N = INT \left(log_{\frac{1-p}{1+p}} \left(\frac{\varepsilon_{cu3}}{\varepsilon_{c3}(1 + p)} \right) + 1 \right). \tag{20}$$

3.4 Saw-Tooth Laws for Steel in Tension and Compression

An elastic perfectly plastic stress-strain diagram has been adopted for reinforcing steel (for tension and compression), according to EC2 prescriptions [9], see Fig. 3b. The procedure adopted is identical to the one used for concrete in compression, with the only difference that in the case of steel the same constitutive law will hold for tension and compression:

$$\sigma^+ = (1 + p)f_y \tag{21}$$

Where, f_y is the yield strength and p the percentage of strength uplifting. The intersection between generic i secant elastic branch and the post peak plastic plateau is given by the following equation:

$$E_i \varepsilon_i^+ = (1 + p)f_y \tag{22}$$

Therefore, analogously to Eq. (11):

$$\varepsilon_i^+ = \frac{(1+p)f_y}{E_i} \qquad (23)$$

Finally, the updated (i.e. degraded) Young's modulus becomes:

$$E_{i+1} = \frac{(1+p)f_y - 2pf_y}{\varepsilon_j^+} = \frac{f_{yi}^-}{\varepsilon_j^+} = E_j \frac{1-p}{1+p}; \qquad (24)$$

$$0 \le i \le N$$

Also in this case is necessary to limit the ultimate strain of the saw-tooth diagram according to the mother curve. Consequently, the number of teeth becomes:

$$N = INT\left(log_{\frac{1-p}{1+p}}\left(\frac{\varepsilon_u}{\varepsilon_y(1+p)} \right) + 1 \right) \qquad (25)$$

Note that since the reinforcement is modeled with one-dimensional truss elements, the index i alone is sufficient to quantify the damage level in both tension and compression.

3.5 Orthotropic Fixed Cracking

The stepwise reduction of Young's modulus, as described in the previous sections, in fact implies that the stiffness is reduced in all directions, i.e. stepwise isotropic degradation occurs. Although this isotropy assumption may work for cases of localized fracture in unreinforced conditions, a substantial improvement is necessary when dealing with reinforced concrete [10]. Then, compressive struts develop parallel to the cracks, and the assumption of isotropy does not hold.

Therefore, in analogy to the pioneering approach of Rashid [11], the initial isotropic stress-strain law can be replaced by an orthotropic law upon crack formation. The axes of orthotropy are determined according to a condition of crack initiation, being n the direction normal to the crack plane, and t the direction of the compressive struts (i.e. tangential to the crack plane). As far as the present work concerns, the crack plane is kept fixed after the crack is nucleated.

Referring to the plane stress situation, and to a local n,t coordinate system oriented along the crack plane, the following constitutive relation is assumed e.g. [12]:

$$\begin{Bmatrix} \sigma_{nn} \\ \sigma_{tt} \\ \sigma_{nt} \end{Bmatrix} = \begin{bmatrix} \dfrac{E_i \cdot E_j}{E_j - v^2 \cdot E_i} & \dfrac{v \cdot E_i \cdot E_j}{E_j - v^2 \cdot E_i} & 0 \\ \dfrac{v \cdot E_i \cdot E_j}{E_j - v^2 \cdot E_i} & \dfrac{E_j^2}{E_j - v^2 \cdot E_i} & 0 \\ 0 & 0 & \beta \cdot G \end{bmatrix} \begin{Bmatrix} \varepsilon_{nn} \\ \varepsilon_{tt} \\ \varepsilon_{nt} \end{Bmatrix} \qquad (26)$$

where E_i the reduced Young's modulus in tension along the n-axis and E_j the reduced Young's modulus in compression along the t-axis according to the above sequentially linear scheme. Moreover, β is the so-called shear retention factor and G is the initial shear modulus. The equation can be rewritten in compact form as follows:

$$\sigma_{nt} = D_{nt}\varepsilon_{nt} \qquad (27)$$

Given the following transformations for the strain and stress vectors:

$$\begin{cases} \varepsilon_{nt} = T_\varepsilon(\phi)\varepsilon_{xy} \\ \sigma_{nt} = T_\sigma(\phi)\sigma_{xy} \end{cases} \qquad (28)$$

Eq. 27 can be easily transposed in terms of stress and strain global components by pre- and post-multiplication with the transformation matrices:

$$\sigma_{xy} = T_\sigma^{-1}(\phi)D_{ns}T_\varepsilon(\phi)\varepsilon_{xy} \qquad (29)$$

The above orthotropic scheme combines the different saw-tooth laws for concrete in tension and compression, and was implemented in the overall event-by-event procedure.

4 SOME APPLICATIONS TO REINFORCED CONCRETE STRUCTURES

Various reinforced structures are considered in this Section. Every structure has been modeled by four-noded plane stress elements for the concrete and two-noded truss elements for the reinforcement. Perfect bond was assumed between the concrete and reinforcement. All the sequentially linear analyses have been performed by choosing a strength range percentage $p=10\%$. Comparisons are made both in terms of load-displacement curve and crack patterns.
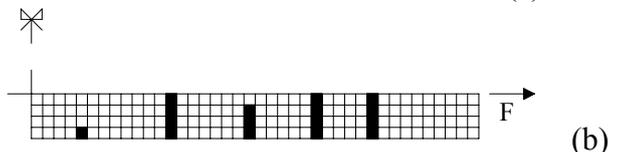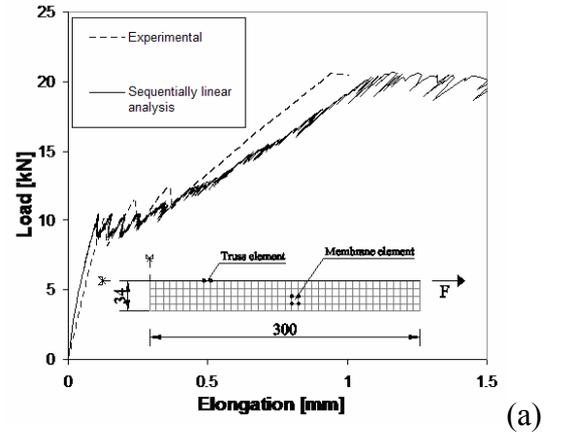
Figure 4. Load-elongation response for tension-pull specimen (a); crack pattern (b).

4.1 *Reinforced tension-pull specimen*

A long-embedment tension-pull specimen is considered [13]. The specimen is 600 mm long and the square transversal section is 68x68mm, reinforced with a Φ8mm rebar. The concrete parameters were: Young's modulus E = 28000 MPa, Poisson's ratio ν = 0.2, tensile strength f_{ct}=2.5 MPa, fracture energy G_F = 60N/m, shear retention factor β = 0.2. The reinforcing bar was given a Young's modulus E_s = 192300 MPa, and a yield stress f_{sy} = 400 MPa. Fig. 4a shows the numerical results obtained using the saw-tooth tension softening curve of Fig. 2.

The sequentially linear analysis shows about five local peaks associated with the subsequent development of five primary cracks. Beyond these peaks snap-backs appear automatically (Fig. 4). The behavior is remarkably similar to the experiment where vertical jumps occur due to the use of displacement-control. Precise quantitative comparisons have not been made, as this would require bond-slip to be included. The analysis also demonstrates that reinforcement plasticity is captured correctly, due to the use of the saw-tooth curve of Fig. 3b for the steel.

4.2 *Reinforced concrete deep beam*

The deep RC beams, experimentally tested by Braam [14], have been analyzed. Beam #13 was loaded in four-point bending with a span of 5m. The beam was 5.5m long with rectangular transverse cross section (300x800mm).
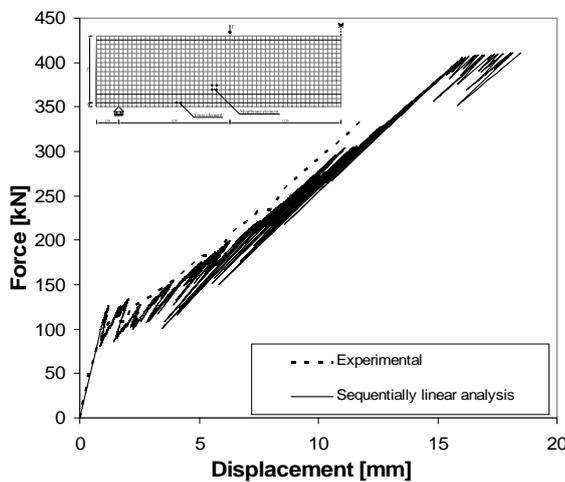
Figure 5. Comparison between experimental and numerical results for beam#13.

The saw-tooth non-linear tension softening curve has been adopted for concrete in tension and a saw-tooth elastic-plastic diagram for steel. Mechanical properties adopted for concrete are the following: Young's modulus E_c = 32000 MPa, Poisson's ratio ν = 0.2, tensile strength f_{ct} = 3 MPa, energy fracture G_F = 60 N/m. The longitudinal reinforcement of beam#13 is constituted of 4Φ20mm, the adopted Young's modulus E_s = 200000 MPa and the steel yielding is equal to f_{sy} = 566 MPa.
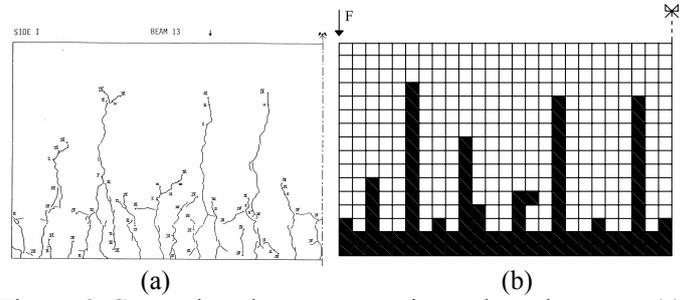
Figure 6. Comparison between experimental crack pattern (a) and the contour of concrete elements which reach complete damage on their final saw-tooth (b) for beam#13.

Fig. 5 shows the comparison between experimental and numerical results in terms of applied load versus midspan deflection. The aim of experimental tests was to investigate the behavior at the serviceability limit state, so measurements have been stopped before the ultimate load was reached, while numerical results continue until the collapse mechanism occurs due to yielding of rebars.

Fig. 6 shows, for the zone between the point of application of the load and the midspan of beam#13, the comparison between experimental crack pattern and the contour of concrete elements which reach the complete damage, (i.e. the maximum number of teeth N). The localized cracking pattern accompanied by local peaks and snap-backs in the load-displacement response is reproduced correctly. Please note that this behavior is obtained fully automatically, as a sequence of linear analyses. This approach always converges as the secant system matrix is always positive definite. Incremental-iterative nonlinear procedures would encounter difficulties or even divergence, especially in the early stage of brittle snap-back cracking.

4.3 *Reinforced concrete deep beam on three supports*

DWT2 beam, tested by Leonhardt and Walther [15], has been chosen for the numerical simulation with DIANA nonlinear models and with sequentially linear analysis. This beam is a two span deep beam, of length 3040 mm, depth 1600 mm, and constant thickness equal to 100 mm, with a 360 mm thick supporting member in the middle (Fig. 7a).

In the experimental test, the failure of DWT2 deep beam occurred at the ultimate load equal to 2462 kN, but the measurements were performed up to a load level of 2200 kN.

4.3.1 *NLFE analysis*

Exploiting symmetry, only one half of the beam has been analyzed. Fig. 7b shows that also support platens have been modeled by steel membrane elements, rigidly fixed to the concrete elements.

NLFE analyses have been carried out with DIANA. A fixed smeared crack model, based on the concept of total-strain, was employed. The compres-

sion non-linearity of the concrete has been ignored. Only tensile cracking has been included and elastic-plastic behavior of the reinforcement.

(a)   (b)
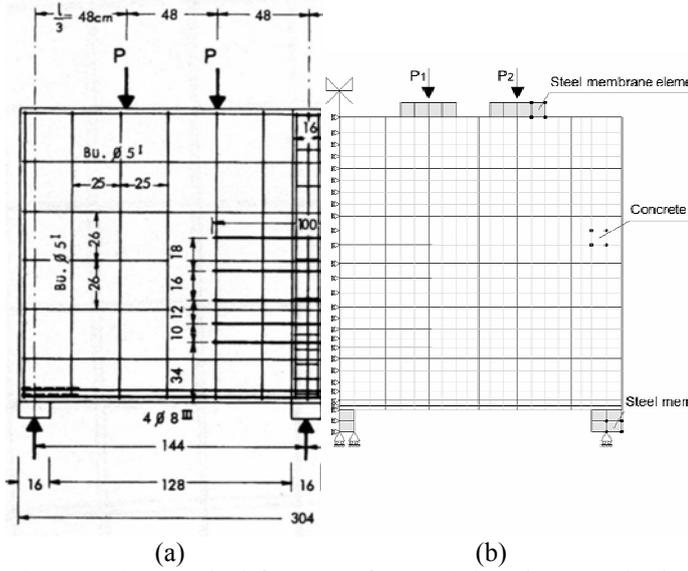
Figure 7. Geometrical features of DWT2 deep beam and reinforcement arrangement [15] (dimension in cm.) (a). Element mesh with details of the support platens (b).

The mechanisms that transmit forces across cracks in RC have been modeled by an average tension-stiffening stress-strain relationship for concrete in tension. The usual assumption is that the stress carrying capacity of the reinforced concrete gradually decreases and is exhausted once the reinforcement starts yielding. This implies that the ultimate strain w_c/h of the proposed tension-stiffening curve equals the yield strain f_y of the steel rebars. The nonlinear curve of Fig. 1 has been approximated as close as possible by adopting DIANA's multi-linear option. A constant shear retention factor equal to $\beta = 0.2$ describes the shear behavior of fixed cracks. The load-deflection curve obtained with the NLFE analysis (Fig. 8) exhibits a very sudden drop in step 30. Here, the NLFE analysis diverged when a full tangent stiffness scheme based on the local negative softening slopes was employed.
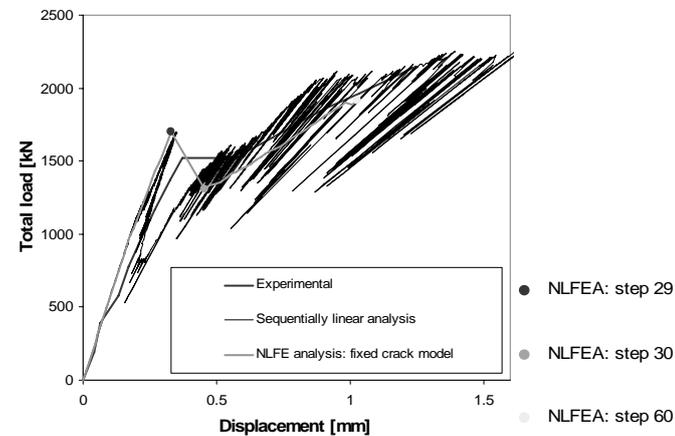
Figure 8., Load-deflection diagram.

(a)   (b)
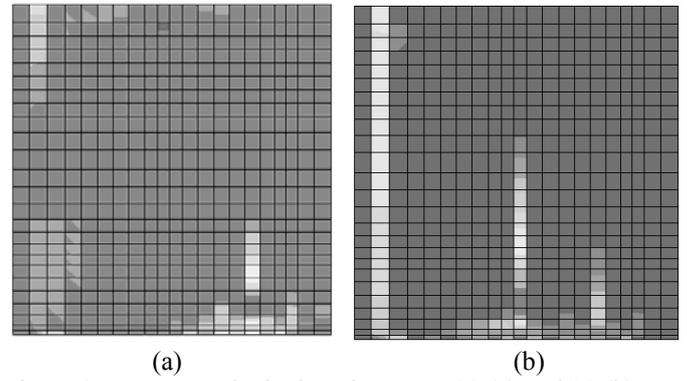
Figure 9. NLFEA: principal strain at step 29 (a) and 30 (b).

(a)   (b)
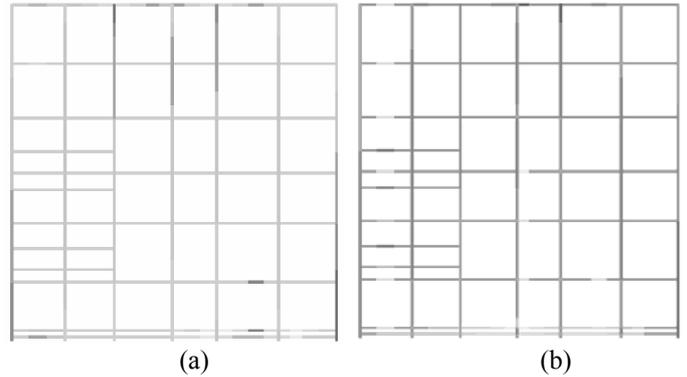
Figure 10. NLFEA: steel stress at step 29 (a) and 30 (b).

Only by using a non-consistent tangent stiffness, at structural level, based upon the positive secant stiffness of the stress-strain curves at local level, the analysis could be continued, though still 'insufficient convergence' occurred. The convergence has not been reached after 100 iterations in increment step 30. In this increment step, a crack besides the supporting member suddenly appears, as shown in Fig. 9, where the principal strains and crack patterns are contoured, respectively. At the same time, yielding of the reinforcement Φ5 Type I occurs over the middle support, Fig. 10.

(a)   (b)
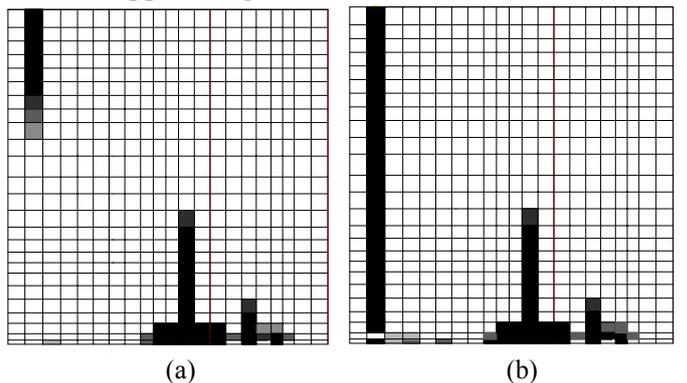
Figure 11. Sequentially linear analysis: concrete damaged element at total load F=1620 kN just before snap-back (a), at F=752 kN in the valley of the snap-back (b).

Beyond this critical point, the analysis could be partially continued and the cracks become wider. The conclusion is that the standard incremental-iterative Newton-Raphson procedure is not capable of adequately catching the sudden, explosive cracking that occurred in the experiment.

4.3.2 *Sequentially linear analysis*

As an alternative, the same beam with the same parameters was analyzed in the sequentially linear fashion. Saw-tooth approximations have been adopted for the non-linear tension softening curve for concrete in tension and for the elastic-plastic diagram for steel.

It is important to note that the experimental test has been carried out in load control while NLFE and sequentially linear analyses have been carried out in displacement control. For this reason the experimental curve shows a flat plateau in the zone where the NLFE analysis diverges. The sequentially linear analysis clearly reveals what happens): it shows a pronounced quasi-static snap-back behavior (Fig. 8) revealing the very sudden and brittle development of the major vertical crack(s) near the mid-support. This snap-back and also other ripples appear automatically due to the scaling procedure.
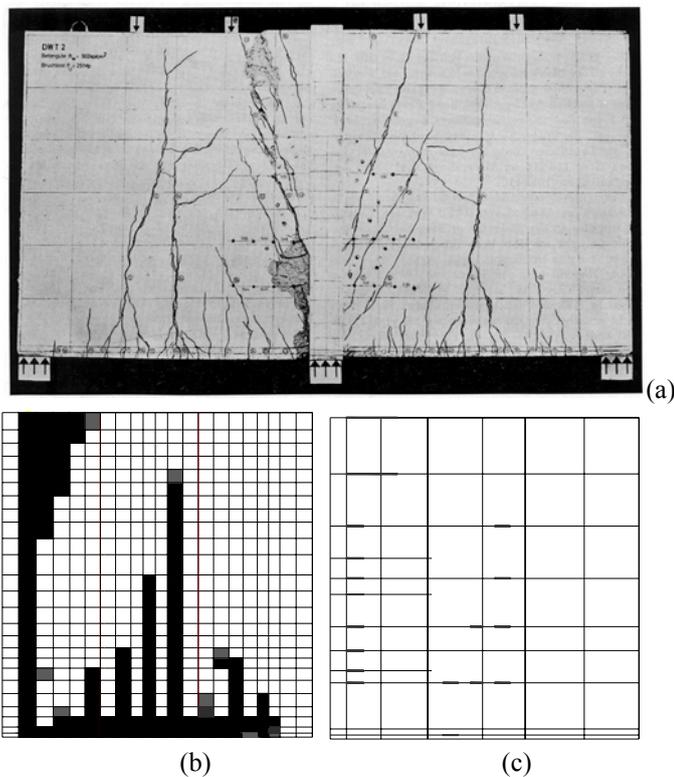
Figure 12. Experimental crack pattern (a), sequentially linear analysis: concrete damaged elements (b) and steel yielded elements (c) at final load F=1930 kN.

Fig. 12a shows the experimental crack pattern at failure. Figs. 12b show, in black, concrete elements which reach the complete damage (i.e. the maximum number of teeth N), respectively for deflection values equivalent to increment steps 29, 30 considered for NLFE analysis, and close to failure. In Fig. 12c yielded steel element are indicated in red.

5 CONCLUSIONS

A sequentially linear method for the analysis of RC structures has been presented. The method replaces softening curves of negative downward slope by positive secant slopes using a saw-tooth rippled stress-strain diagram, both for concrete in tension, concrete in compression and steel in tension and compression. Results prove that the model is capable of simulating brittle snap-back type of cracking (typical for RC) as well as ductile plastic response. The approach always 'converges' as the secant saw-tooth stiffness is always positive definite. The approach is stable and robust and therefore appealing to practicing engineers. Future developments are required, e.g. towards non-proportional loading.

REFERENCES

Carpinteri A. Interpretation of the Griffith instability as a bifurcation of the global equilibrium, in NATO Advanced Workshop on Application of Fracture Mechanics to Cementitious Composites, Ed. P. Shah, Martinus Nijhoff, 1984: 287-316.

De Borst R. Computation of post-bifurcation and post-failure behaviour of strain-softening solids. Computers and Structures, 1987; 25(2): 211-224.

Crisfield MA. Accelerated solution techniques and concrete cracking. Computer Methods in Applied Mechanics and Engineering, 1982, 33: 585-607.

Rots JG. Sequentially linear continuum model for concrete fracture. In Fracture Mechanics of Concrete Structures, de Borst R, Mazars J, Pijaudier-Cabot G, van Mier JGM, Balkema AA (eds). Lisse: The Netherlands, 2001, 831-839.

Rots JG, Invernizzi S. Regularized sequentially linear saw-tooth softening model. Int. Journal for Numerical and Analytical Methods in Geomechanics, 2004, 28: 821-856.

Rots JG, Invernizzi S, Belletti B, Saw-tooth softening/stiffening – a stable computational procedure for RC structures. Computers & Concrete, 2006, 3(4):213-233.

CEB-FIB Model Code 1990. Bulletin No. 213/214 (1993), Comite International du Beton.

Belletti B, Cerioni R, Iori I. Physical approach for reinforced concrete (PARC) membrane elements. ASCE Journal of Structural Engineering, 2001, 127 (12): 1412-26.

Eurocode 2: Design of concrete structuree – Part 1: General rules and rules for buildings. CEN, 2002.

Rots JG, Invernizzi S. Saw-tooth softening/stiffening model, in Fracture Mechanics of Concrete Structures, (eds. V.C. Li, C.K.Y. Leung, K.J. William, S.L. Billington), USA, 2004, 1:375-382.

Rashid YR. Analysis of prestressed concrete pressure vessels. Nuclear Engng. And Design, 1968, 7(4): 334-344.

Rots JG, Nauta P, Kusters GMA, Blaauwendraad L. Smeared crack approach and fracture localization in concrete. HERON, 1985, 30(1):1-48.

Gijsbers FBJ, Hehemann AA. Some tensile tests on reinforced concrete. TNO-IBBC Report BI-77-61, Rijswijk, 1977.

Braam CR. The behavior of deep reinforced concrete beams – Experimental results. Report 25-5.90.5/VFA-2, Stevin Laboratory, Delft University of Technology, Delft, 1990.

Leonhardt F., and Walter R. Wandartige Trager. Deutsher Ausschuss für Stahlbeton, D.A.f. St., Heft 178, Ernst & Sohn, Berlin, Germay, 1966.